A DNS STUDY OF EFFECTS OF REYNOLDS NUMBER ON UNSTEADY CHANNEL FLOW

S. He and M. Seddighi
Department of Mechanical Engineering
University of Sheffield
Sheffield S1 3JD, United Kingdom
s.he@sheffield.ac.uk, seddighi@sheffield.ac.uk

ABSTRACT

We have previously shown that the response of turbulence in a transient channel flow is effectively a laminar-turbulent bypass transition. In that study, only one step-change flow between fixed initial and final Reynolds numbers was investigated. This paper reports a series of new simulations with a range of initial and final Reynolds numbers. All cases studied show characteristics of transition. The main effect of varying the Reynolds number can be attributed to the change of the 'free-stream' turbulence intensity and the critical equivalent Reynolds numbers of all cases are well correlated with a simple function of the initial turbulence intensity.

1. INTRODUCTION

In a recent DNS study of the transient channel flow following a sudden increase of flow rate of an initially turbulent flow (He & Seddighi 2013, referred to as HS2013 hereafter), we have shown that a low-Reynolds-number turbulent flow can undergo a process of transition that resembles the laminar-turbulent transition. In response to the rapid increase of flowrate, the flow does not progressively evolve from the initial turbulent structure to a new one, but undergoes a process involving three distinct phases (pre-transition, transition and fully turbulence) that are equivalent to the three regions of the boundary layer bypass transition, namely, the buffeted laminar flow, the intermittent flow and the fully turbulent flow regions. This transient channel flow represents an alternative bypass transition scenario to the free-stream turbulence (FST) induced transition, whereby the initial flow serving as the disturbances is a low-Reynolds-number turbulent wall shear flow with pre-existing streaky structures. A thin boundary layer of high strain rate is formed adjacent to the wall following the rapid increase of flow rate, which grows into the core of the flow with time providing the main reasons for further changes of the flow. The pre-existing turbulent structures act as background perturbations to this boundary layer, much like the role that the free stream turbulence plays in a bypass transition. These turbulent structures are modulated by the time-developing boundary layer and stretched to produce elongated streaks of high and low streamwise velocities, which remain stable in the pre-transitional period. At this stage, the axial fluctuating velocity increases steadily but the other two components remain effectively unchanged. In the transitional phase, localised turbulent spots are being generated which are distributed randomly in space. Such turbulent spots grow longitudinally as well as in the spanwise direction, merging with each other and eventually occupying the entire wall surfaces when the transition completes and the flow becomes fully turbulent.

In HS2013, only one case was considered, whereby the initial and the final Reynolds numbers ($Re_b = U_b \delta / \nu$, where U_b is the bulk velocity of the flow and δ the half channel height) were 2800 and 7400 respectively. The purpose of the study reported herein is to investigate the effect of the initial and final Reynolds numbers on the characteristics of the response of turbulence. A summary of the test conditions is shown in Table 1.

For recent progresses in research in unsteady channel/pipe flows, the readers are referred to He & Jackson (2000), Greenblatt & Moss (2004) and Chung (2005). Many studies have been conducted on bypass transition, e.g., Jacobs & Durbin (2001) and Matsubara & Alfredsson (2001). Of particular interest are those investigated into the effects of free-stream turbulence intensity and length scales on transition, e.g., Andersson et al (1999), Brandt et al (2004), Fransson et al (2005), Ovchinikov et al (2008) and Vaughan & Zaki (2011).

2. METHLOGY

The simulations are performed using an "in-house" code. A second order finite difference method is used to discretize the spatial derivatives of the governing equations on a rectangular grid. An explicit Runge-Kutta together with an implicit Crank-Nicholson scheme is incorporated into the fractional-step method. The Poisson equation for the pressure is solved by an efficient 2-D FFT. The equations are solved in a domain of $18\delta \times 2\delta \times 5\delta$, with a mesh of ($1024 \times 240 \times 480$) in the streamwise ($x$), normal ($y$), and spanwise ($z$) directions, respectively. The Message-Passing Interface (MPI) is used to parallelize the code which is validated for steady channel flow results against well-known DNS database.

For any simulation, the flow starts from a fully developed steady turbulent flow and is rapidly increased to reach the final Reynolds number and the simulation then continues until a new steady flow is reached.

1

3. RESULTS AND DISCUSSION

3.1 The general picture

Figure 1 shows three-dimensional iso-surface plots of $u'/U_{b1}=\pm0.35$ and $\lambda_2 =-7$ in RE16 (Re_b=2800 to 12600). In comparison with RE01 (studied in HS2013), the Re_{b0} is the same but Re_{b1} is much higher than 7400 used in RE01. In the figure, λ_2 is the second largest eigenvalue of the symmetric tensor $S^2 + \Omega^2$ where S and Ω are the symmetric and antisymmetric parts of the velocity gradient tensor ∇u. It is clear that the basic features of the flow exhibited in this figure are consistent with that found in HS2013 and summarised in the Introduction. Initially in the pre-transitional stage (t^*<20, where $t^* = t/(\delta/U_{b1})$), the iso-surfaces of u'/U_{b1} form long tubes which appear alternatively, clearly showing elongated streaks similar to those identified in boundary layer bypass transitions. These iso-surface tubes break up alongside the generation turbulent spots as transition progresses. Hairpin vortical structures are clearly identifiable through the iso-surface of λ_2. There are fewer such structures in the early pre-transitional stage but many start to appear from the late pre-transition and transition stages. The vortices often occur around the low-speed streaks accompanying their breakup, which is similar to those shown in boundary layer bypass transition.

Figure 2 shows the variation of the friction coefficient ($c_f = \frac{\tau_w}{\frac{1}{2}\rho U_{b1}^2}$) in the various cases investigated in this study. Focusing on case RE16, it can be seen that the c_f increases rapidly following the commencement of the excursion due to the inertia resulting from the rapid flow acceleration, but decreases quickly until about t^*=12 where it reaches a minimum, after which it increases quickly to around the final steady value. Comparing with the flow visualisation of the corresponding test case, it is clear that the timing of the minimum c_f coincides with the onset of the transition (referred to as the critical time, t^*_{cr}) and the decrease of c_f before this time follows a behaviour that can be described by the Blasius solution for a laminar boundary layer.

3.2 Effect of starting and final Reynolds numbers

The effect of varying the starting and final Reynolds numbers on the overall flow behaviour can be studied by investigating the development of the friction coefficient. It is clear from figure 2(a) that t*$_{cr}$ reduces monotonically with the increase of the Re_{b0}. For a fixed Re_{b1} of 7400, the non-dimensional time t^*_{cr} reduces from 20 to 8 when Re_0 is increased from 2800 to 5300. In addition, alongside the reduction of t*$_{cr}$, the minimum friction coefficient increases significantly, showing a progressively smaller 'undershooting' at the final c_f. It is also interesting to note that although the initial c_f is quite different in the various cases due to the different starting Re, the evolution of c_f with t^* in the early stage does not differ significantly.

Figure 2(b) shows that increasing Re_{b1} results in a reduction in t*$_{cr}$. For a fixed Re_{b0} of 2800, as Re_{b1} is increased from 3100 to 12600, t^*_{cr} increases from 12 to 32. In addition, the minimum c_f varies from a very small 'undershooting' at Re_{b1}=3100 to a strong one at Re_{b1}= 12600. The final c_f reduces with the increasing of Re_{b1}.

The behaviour of the friction in transient channel flow can be compared with that in boundary layer bypass transition. To do this, it is necessary to define an equivalent Reynolds number based on the axial distance x, which can be defined as the distance that a particle travels after the start of the flow transient. This can be related to the time elapse through a convection velocity, which is likely to be proportional to the bulk velocity, though the proportionality may be dependent on the particular flow. Here, for simplicity, we use U_{b1} as the characteristic convective velocity, i.e., $x = tU_{b1}$. Consequently, the equivalent Reynolds number can be expressed as:

$$Re_x = \frac{xU_{b1}}{\nu} = \frac{tU_{b1}^2}{\nu} \tag{1}$$

Since $t^* = t/(\delta/U_{b1})$ and $Re_{b1} = \frac{\delta U_{b1}}{\nu}$, we have

$$Re_x = t^* Re_{b1} \tag{2}$$

The data shown in Figure 2 are re-plotted in Figure 3 with respect of Re_x. According to Equation 2, for any test cases of the same Re_{b1}, $Re_{x,cr}$ and t^*_{cr} are directly proportional to each other, and hence figures 3(a) and 4(a) are similar. When Re_{b0} is fixed, however, the increase of $Re_{x,cr}$ is much greater than t^*_{cr} as Re_{b1} is increased, which can be clearly observed in Figures 3(b).

The mechanisms by which the starting and final Reynolds numbers affect the transition process (and the critical equivalent Re) are no doubt very complex. Below are some plausible factors to be considered:

(i) Re_{b0} (= $\delta U_{b0}/\nu$) defines the initial turbulence in terms of amplitude and time/length scales. The higher the Re_{b0}, the higher the initial turbulence intensity but also the smaller the time/length scales. It also defines the initial mean velocity profile.

(ii) Re_{b1} defines the 'free stream' velocity. Arguably this is the most important velocity of the transient flow.

(iii) (Re_{b1}-Re_{b0}), which defines Ub_1-Ub_0, is the cause of the change. And indeed, the time-developing boundary layer is characterized by this velocity.

(iv) The acceleration rate could potentially be a factor. Here, the acceleration is very rapid and the flow increase can be viewed as a step change. Tests with the acceleration rate increased by an order of magnitude show no effect. For a transient with a much slower rate, the acceleration does affect the response. Results are reported elsewhere.

(v) The 'free-stream' turbulent intensity is dependent on both Re_{b0} and Re_{b1}, which can be written as u'_0/U_{b1}.

We have investigated the various mechanisms discussed above and correlated the data against alternative parameters. It has become evident that the main effect of Re_{b0} and Re_{b1} on the critical Reynolds number is through changing the initial/'free-stream' turbulence intensity.

Turbulence in a fully developed channel is very different from the free-stream turbulence of the boundary layer, being highly anisotropic and spatially non-uniform. We use the peak values to characterise the turbulence intensity, that is:

$$Tu_0 = \frac{\sqrt{(u_0'^2+v_0'^2+w_0'^2)/3}}{U_{b1}} \tag{3}$$

which can be written as

$$Tu_0 = \sqrt{(u_0'^{+2} + v_0'^{+2} + w_0'^{+2})/3}\left(\frac{u_{\tau 0}}{U_{b1}}\right) \quad (4)$$

In the Reynolds number range considered here, the peak values of the three r.m.s. turbulent fluctuating velocities are around 2.7, 1.2 and 0.9, respectively. Hence, $Tu_0 \approx 1.8\left(\frac{u_{\tau 0}}{U_{b1}}\right)$. Further noting that $\frac{u_\tau}{U_b}$ is in the range of 16 ~ 18 for the Reynolds numbers considered here, we finally characterize the turbulence intensity as follows:

$$Tu_0 \approx 0.1\left(\frac{U_{b0}}{U_{b1}}\right) \quad (5)$$

Figure 4 shows the critical Reynolds number obtained from Figures 3 (c & d) against the initial turbulence intensity defined above. It can be seen that the data can be well represented by the following expression:

$$Re_{x,cr} = 576Tu_0^{-1.71} \quad (6)$$

Or simply,

$$Re_{x,cr} = 30,000\left(\frac{U_{b0}}{U_{b1}}\right)^{-1.71} \quad (7)$$

The above result shows that the effect of varying the Re_{b0} and Re_{b1} comes down to the variation of the initial turbulence intensity. All other factors discussed above in the list are insignificant as far as the critical Reynolds number is concerned. It has been established through both theoretical and experimental investigations that for spatially developing boundary, $Re_{cr} \sim Tu^2$ (Andersson et al (1999), Brandt et al (2004), Fransson et al (2005), Ovchinikov et al (2008)). In particular, Andersson et al (1999) proposed:

$$Re_{x,cr} = 144\,Tu_0^{-2} \quad (8)$$

Equations 6 and 8 are similar in form but both the multiplier and the exponent are different. The multiplier in equation 6 is more than double that of the bypass correlation. But this is probably a trivial difference because (i) the $Re_{x,cr}$ of the transient flow is based on U_{b1} rather than a carefully defined convection velocity. In HS2013 for example, the convection velocity was found to be 0.74 U_{b1}. This value is not used here because the determination of the ratio involves some arbitrariness; (ii) the initial turbulence in a channel flow is anisotropic and spatial non-uniform. We have used the peak values to define turbulence intensity for convenience and unambiguity but clearly this approach involves certain element of arbitrariness. In contrast, in the wind tunnel boundary layer however, the flow is often isotropic and spatially uniform. This difference in Tu_0 contributes to the difference in the multipliers in Equations 6 and 8.

The difference in the exponents in Equations 6 & 8, although rather small, is probably more significant. Equation 6 can be re-written in terms a Reynolds number based on the initial velocity ($Re_{x0} = tU_{b0}^2/\nu$) as follows,

$$Re_{x0,cr} = 576Tu_0^{0.29} \quad (9)$$

That is, $Re_{x0,cr}$ is a function of the ratio of the initial and the final Reynolds numbers, despite the dependence is weak. Equation 8, however, implies that $Re_{b0,cr}$ is a constant in any transient flows, completely independent of the final Reynolds number. Later, we will show that this is not strictly correct. Nevertheless, Equation 8 is shown in Figure 4 to for a direct comparison with our DNS data. The critical Reynolds number in this equation is multiplied by a factor of 0.6 to bring them to a level similar to that of our data. It can be seen that the boundary layer bypass transition correlation predicts a steeper change in the critical Reynolds number in the lower Tu_0 region. Also shown in the figure is Driest & Blumer (1963) correlation for boundary layer transition,

$$\frac{1}{\sqrt{Re_{x,cr}}} = a + b\sqrt{Re_{x,cr}}Tu^2 \quad (10)$$

where a=10⁻⁴, b=62.5x10⁻⁸, and Re_{cr} is factored by 0.6.

3.3 The time-developing boundary layer

The initial flow response in a transient channel flow can be described using a time-developing boundary layer as discussed in HS2013. Immediately after the rapid increase in the flow rate, a very thin boundary-layer of high strain rate is formed adjacent to the wall, but the bulk of the flow increases as a solid body with no change in its velocity profile. This boundary layer, which progressively develops into the flow with time, retains the character of a laminar boundary before the onset of transition. The time-developing boundary layer can be studied by examining the perturbing velocity:

$$\bar{u}^{\wedge}(y,t^{+0}) = [\bar{u}(y,t^{+0}) - \bar{u}(y,0)]/[\bar{u}_c(t^{+0}) - \bar{u}_c(0)] \quad (11)$$

where $\bar{u}_c$ is the centreline velocity and $t^{+0} = tu_{\tau 0}^2/\nu$.

The profiles of $\bar{u}^{\wedge}$ at various t^{+0} of all the cases are plotted in Figure 5 against y^{+0}. The profiles at any time t^{+0} are shifted with a distance proportional to t^{+0}. The values of $\bar{u}^{\wedge}$ are scaled with an arbitrary factor, which is the same for all cases. It is clear that the time-developing boundary layer shows strong similarities to the spatially developing boundary layer. The profiles in different cases collapse fairly closely on top of each other for $t^{+0}<100$. It can be derived from this observation that the wall shear stress of $\bar{u}^{\wedge}$ normalized in the manner defined below should collapse on top each other when expressed in terms of t^{+0}:

$$c_{f1} = \frac{\tau_{w,du}}{\frac{1}{2}\rho(U_{b1}-U_{b0})u_{\tau 0}} \quad (12)$$

where $\tau_{w,du} = \{\mu\partial[u(y/\delta,t^*) - u(y/\delta,0)]/\partial y\}|_{y/\delta=0}$. Such a plot is shown in Figure 6. It can be seen that all data indeed collapse on a single curve during the pre-transitional stage. The critical t^{+0} varies somewhat from case to case (80 to 110). This variation is moderate considering the large variation of the Re_{b0} and Re_{b1}

covered. In fact, Equation 8 would imply that t^{+0} is a constant for all cases, whereas the small change of t^{+0} can be predicted by Equation 9, assuming $\frac{u_\tau}{U_b} \sim constant$:

$$t_{cr}^{+0} \propto Tu_0^{0.29} \tag{13}$$

Figure 7 shows the displacement thickness of the differential flow field ($\bar{u}^{\wedge}$) in the various cases. They correlate reasonably well normalized using the initial wall units. The boundary layer thickness and the displacement thickness of RE01 are also shown in Figure 4 to illustrate the general trend of the growth of the boundary layer.

Figure 8 shows the development of the u' and v' in RE14 and RE16, which has the same Re_{b0} but different Re_{b1}. The Reynolds number ratio is 1.1 and 4.5 respectively, representing high and low 'free-stream turbulence'. Although the levels of the increase of u' and v' are very different in the two cases, the following trends are the same in these (and all other) cases: (i) u' increases progressively from the start of the transient, and at the time of the onset of the transition the peak value has reached a level that is close to the maximum value. (ii) In contrast, v' remains largely unchanged (or reduces slightly) during the pre-transition period. It only starts increasing when transition occurs. In HE2013, these flow features were associated with the transition process: the progressive increase of u' immediately reflects the formation and enhancement of the streaky structures and the distinct two-stage response of v' reflects the generation and growth of turbulence spots.

Figure 9 shows the time development of the negative spanwise correlation of u' (i.e., $-R_{11}$) in 8 cases. The top row cases have the same Re_{b1} but different Re_{b0}, whereas the bottom row cases have the same Re_{b0}, but different Re_{b1}. The streaky structures in the pre-transition and the break-up of them are clearly shown in all cases. The intensity shows the strength of the streaky structures, and the location (z/δ) of the peak correlation indicates the half-spacing of the streaks. It is clear that, with the increase of Re_{b0}, the spacing and the strength of the streaks reduce, and t^*_{cr} increases. In contrast, with the increase of Re_{b1}, the spacing and the strength of the streaks and t^*_{cr} all increase. It is of particular interest to note that the main features of the transition exhibited in c_f, turbulent velocities and correlations are very similar in all cases, including a case with an increase of flow of only 10%.

4. CONCLUSIONS

In summary, all cases studied show laminar-turbulent transition. The effect of varying the Reynolds numbers are reflected only through changing the initial turbulence intensity and the critical equivalent Reynolds numbers of all cases are well correlated with a simple function of the initial turbulence intensity.

REFERENCES

Andersson, P., Berggren, M., & Henningson, D.S. 1999. Optimal disturbances and bypass transition in boundary layers. *Physics of Fluids*, 11, (1) 134-150

Brandt, L., Schlatter, P., & Henningson, D.S. 2004. Transition in boundary layers subject to free-stream turbulence. *J. Fluid Mech.*, 517, 167-198

Chung, Y.M. 2005. Unsteady turbulent flow with sudden pressure gradient changes. *International Journal for Numerical Methods in Fluids*, 47, (8-9) 925-930

Fransson, J.H.M., Matsubara, M., & Alfredsson, P.H. 2005. Transition induced by free-stream turbulence. *J. Fluid Mech.*, 527, 1-25

Greenblatt, D. & Moss, E.A. 2004. Rapid temporal acceleration of a turbulent pipe flow. *J. Fluid Mech.*, 514, 65-75

He, S. & Jackson, J.D. 2000. A study of turbulence under conditions of transient flow in a pipe. *J. Fluid Mech.*, 408, 1-38

He, S. and Seddighi, M. 2013 Turbulence in transient channel flow, *J. Fluid Mech.*, 715, 60-102

Jacobs, R.G. & Durbin, P.A. 2001. Simulations of bypass transition. *J. Fluid Mech.*, 428, 185-212

Matsubara, M. & Alfredsson, P.H. 2001. Disturbance growth in boundary layers subjected to free-stream turbulence. *J. Fluid Mech.*, 430, 149-168

Ovchinnikov, V., Choudhari, M.M., & Piomelli, U. 2008. Numerical simulations of boundary-layer bypass transition due to high-amplitude free-stream turbulence. *J. Fluid Mech.*, 613, 135-169

Vaughan, N.J. & Zaki, T.A. 2011. Stability of zero-pressure-gradient boundary layer distorted by unsteady Klebanoff streaks. *J. Fluid Mech.*, 681, 116-153

Van Driest, E. R. & Blumer, C. B. 1963. Boundary layer transition: Free-stream turbulence and pressure gradient effects. *AIAA J.* **1**, 1303.
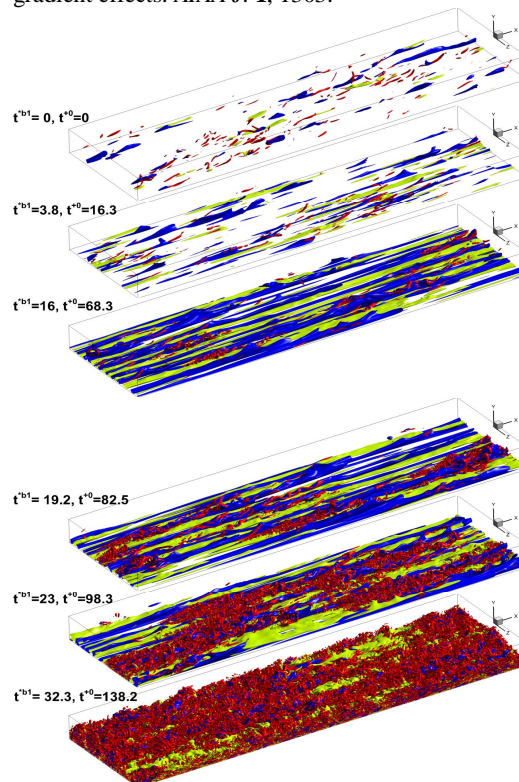
Figure 1 Flow structures in 3D iso-surface plots in RE16 (Re_b=2800 to 12600), Green/Blue: u'=±0.35, Red: λ_2=-7.
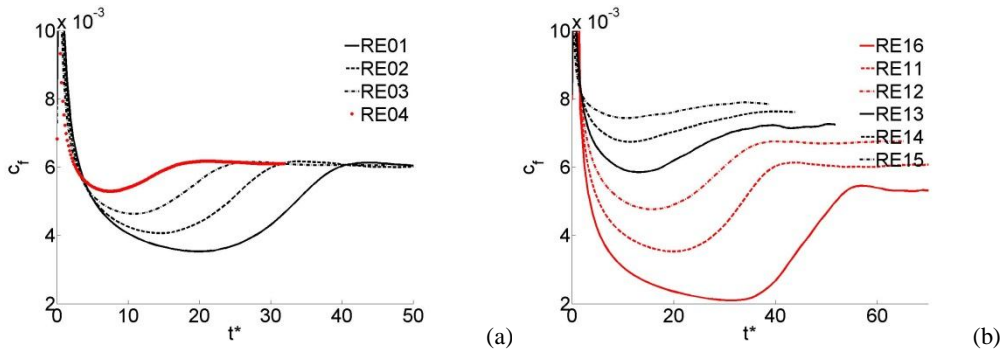
Figure 2 Friction coefficient, (a) Effect of Re_{b0} (same Re_{b1}) (b) Effect of Re_{b1} (same Re_{b0})
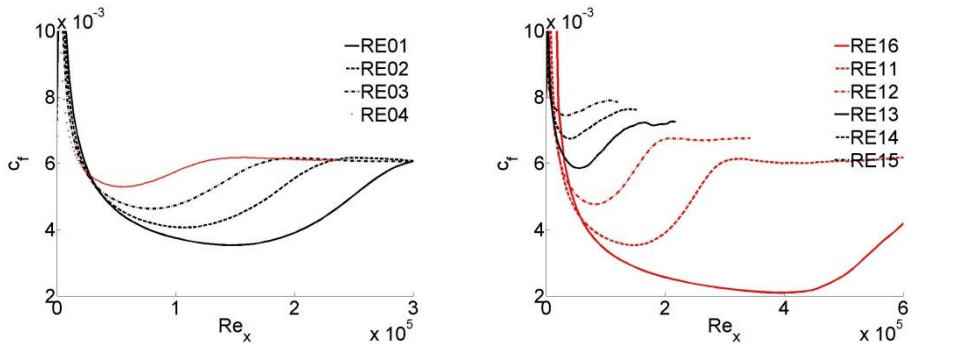

Figure 3 Friction coefficient versus Re_x, (a) Effect of Re_{b0} (same Re_{b1}) (b) Effect of Re_{b1} (same Re_{b0})
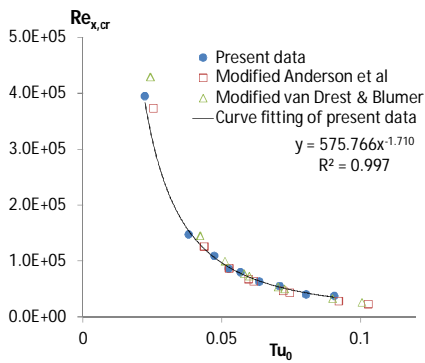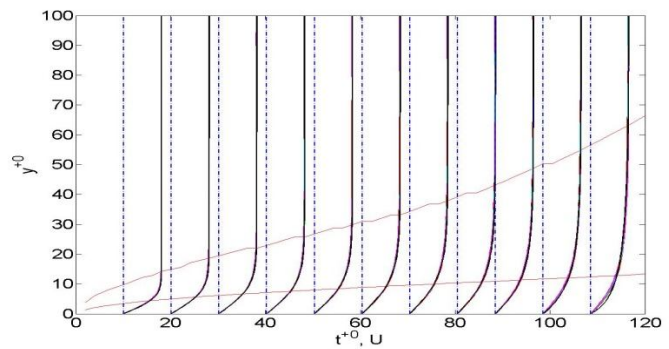

Figure 4 Critical Reynolds number

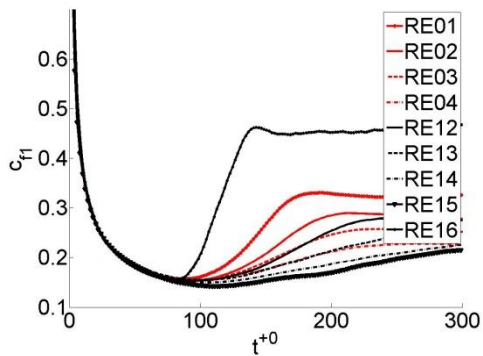Figure 5 Development of the differential velocity profile (u^) in all cases

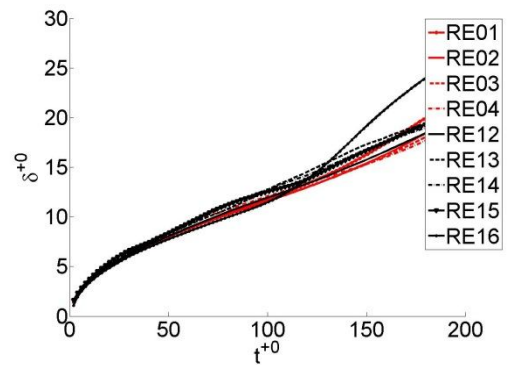

Figure 6 Friction coefficient versus t^{+0} in all cases
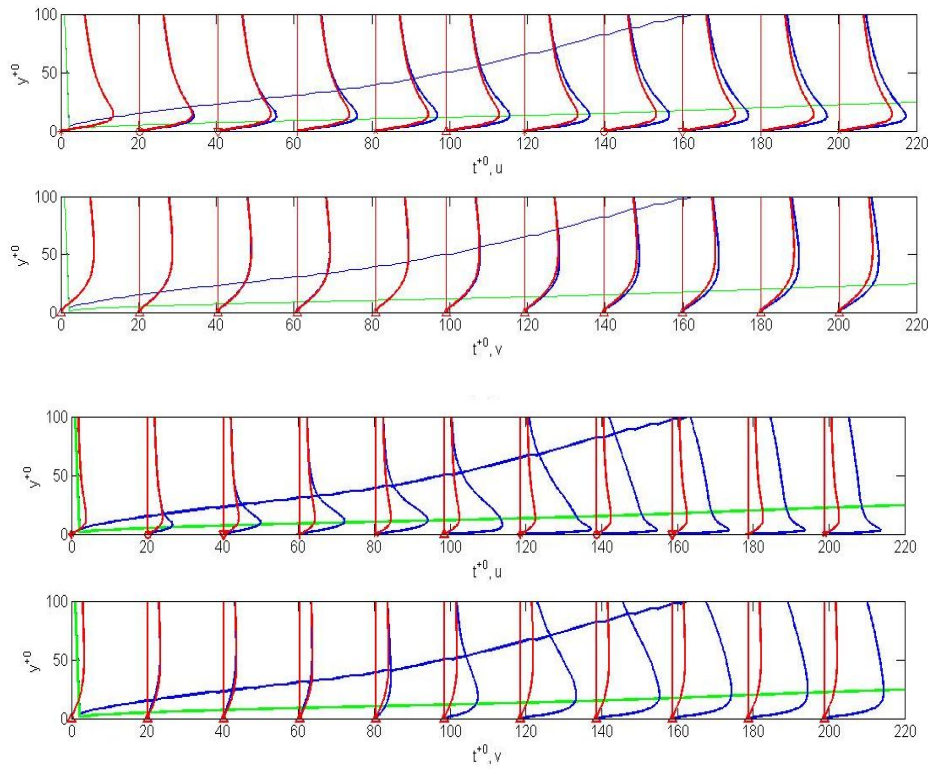
Figure 7 Momentum thickness of u^ profile

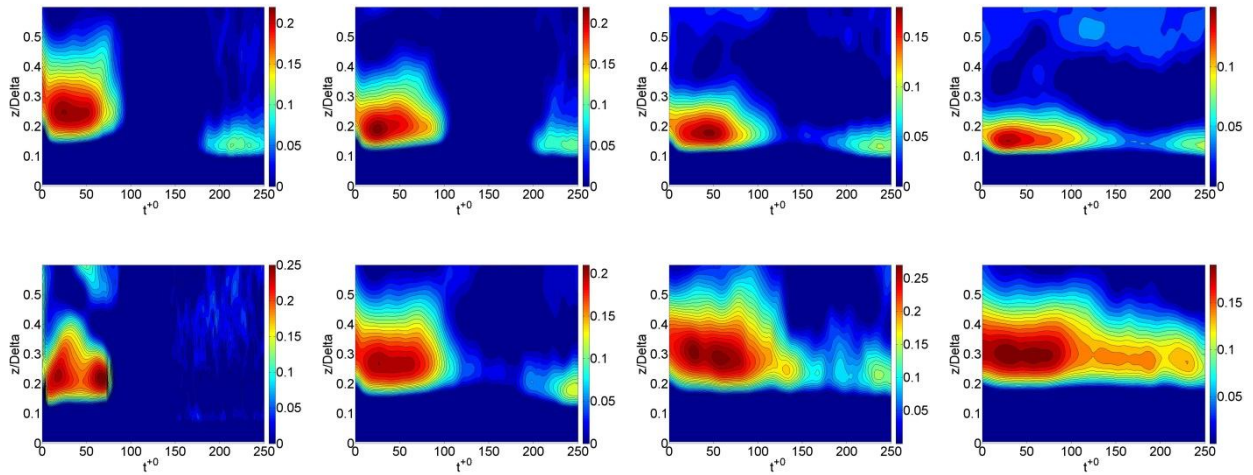Figure 8 The development of u' and v' in (a) RE14 and (b) RE16.

Figure 9 Time variation of the spanwise correlation of the streamwise velocity (magnitudes of negative values are shown, positive values are set to zero); Top: RE01, RE02, RE03, RE04, Bottom: RE16, RE12, RE13, RE14.

Table 1 Unsteady flow cases studied

case	Re_{b0}	Re_{b1}	Δt^*	case	Re_{b0}	Re_{b1}	Δt^*
RE01	2800	7400	0.22	RE11	2800	7400	0.22
RE02	3500	7400	0.18	RE12	2800	5300	0.13
RE03	4200	7400	0.15	RE13	2800	4200	0.08
RE04	5300	7400	0.10	RE14	2800	3500	0.04
				RE15	2800	3100	0.02
	Note: RE01=RE11			RE16	2800	12600	0.46

6